Minimum ignition energy of hydrogen-air mixtures at ambient and cryogenic temperatures

Available online at www.sciencedirect.com

ScienceDirect

journal homepage: www.elsevier.com/locate/he

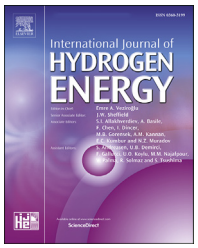

Minimum ignition energy of hydrogen-air mixtures at ambient and cryogenic temperatures

D. Cirrone [a,*], D. Makarov [a], C. Proust [b,c], V. Molkov [a]

[a] HySAFER Centre, Ulster University, BT37 0QB, Newtownabbey, UK
[b] Institut National de L'Environnement Industriel et des Risques, Parc Technologique ALATA, BP2, 60550, Verneuil-en-Halatte, France
[c] Sorbonne University, Laboratory TIMR, UTC/ESCOM, Centre Pierre Guillaumat, 60200, Compiegne, France

HIGHLIGHTS

- Development and validation of model to determine MIE for hydrogen-air mixtures.
- The model is applicable for arbitrary concentration and temperature of the mixture.
- The model employs the laminar flame thickness to calculate a critical flame kernel.
- Effect of flame stretch and preferential diffusion on laminar burning velocity.
- Validation against experiments at ambient and cryogenic temperatures.

ARTICLE INFO

Article history:
Received 27 November 2022
Received in revised form
7 January 2023
Accepted 10 January 2023
Available online 31 January 2023

Keywords:
Hydrogen safety
Spark ignition
Minimum ignition energy
Cryogenic temperatures
Model

ABSTRACT

The ignition and combustion of hydrogen in air is considered more hazardous compared to other fuels due to the lower minimum ignition energy (MIE) and the wider flammability range. Spark discharge is the most common type of electrostatic ignition hazard. There is a need in validated safety engineering tools to accurately calculate MIE in a wide range of temperatures from atmospheric to cryogenic which are characteristic for hydrogen systems and infrastructure. Current MIE assessment methodologies rely on the availability of experimental data on quenching distance and/or laminar burning velocity and thus are mostly empirical correlations. This prevents their application beyond the limited number of experimental data, i.e. to arbitrary composition of the hydrogen-air mixture at arbitrary temperatures including cryogenic. This work aims at the development of a model able to accurately predict MIE for hydrogen-air mixtures with arbitrary initial composition and temperature. Cantera and Chemkin software are used to calculate the properties and unstretched laminar burning velocity of hydrogen-air mixtures. The flame thickness is found to well represent the critical flame kernel in the suggested model. The model is validated against experimental data on MIE for mixtures at ambient and cryogenic (down to 123 K) temperatures. Results show that the effect of flame stretch and preferential diffusion shall be considered to accurately predict MIE for lean hydrogen-air mixtures, which was not possible for previous models.

* Corresponding author.
E-mail address: d.cirrone@ulster.ac.uk (D. Cirrone).

https://doi.org/10.1016/j.ijhydene.2023.01.115

Nomenclature

Acronyms

MIE	Minimum Ignition Energy, J

Greeks

δ_L	Laminar flame thickness, m
δ	Diffusive flame thickness, m
δ_L^0	Thermal flame thickness, m
δ_L^B	Laminar flame thickness calculated using Blint definition, m
δ_L^{BS}	Laminar flame thickness calculated using Blint definition and Sutherland law simplification, m
Φ	Stoichiometric coefficient
ρ	Density, kg/m^3

Latins

C	Capacitance, F
c_p	Specific heat at constant pressure, J/kg/K
d	Diameter of the critical flame kernel, m
E	Energy, J
E_{min}	Minimum energy to ensure ignition, J
k	Thermal conductivity, W/m/K
S	Flame propagation velocity, m/s
S_u	Laminar burning velocity, m/s
S_u^0	Unstretched laminar burning velocity, m/s
S_u^{SD}	Stretched laminar burning velocity accounting for selective diffusion, m/s
T_b	Temperature of burnt mixture, K
T_u	Temperature of unburnt mixture, K
V	Voltage, V
X_{SD}	Parameter of the effect of flame stretch and preferential diffusion on the laminar burning velocity

Subscripts

av	Averaged between parameter value for burnt and unburnt properties
b	Burnt mixture
L	Laminar
u	Unburnt mixture

Superscripts

0	Parameter referring to unstretched laminar burning velocity
B	Blint definition for laminar flame thickness
BS	Blint definition and Sutherland law simplification for laminar flame thickness
SD	Parameter accounting for flame stretch and selective diffusion

Introduction

Hydrogen release into air can easily be ignited due to the lower minimum ignition energy (MIE) and propagate flame due to the wider flammability range of 4–75% of hydrogen in air by volume compared to other fuels. If MIE is usually greater than 100 μJ for flammable gases such as methane or ethane, MIE for hydrogen in air in standard conditions is as low as 17 μJ [1]. Therefore, the ignition potential for hydrogen-air mixtures can be considered greater than for other fuels. The content of oxygen in the mixture affects the value of MIE, causing its decrease to 5.7 μJ for air enriched by oxygen to 35% vol [2]. In experiments with hydrogen combustion in oxygen, it was not possible to measure the MIE due to the limited capability of the experimental apparatus with minimum measurable energy of 4 μJ. The authors of [3] reported that the ignition energy of hydrogen-oxygen can be as low as 1.2 μJ.

The conventional experimental technique to determine the MIE for flammable mixtures is a spark capacitive discharge [2]. From the safety point of view, an investigation of a spark discharge is of great interest as it is the most common type of electric discharge associated to ignition hazards [4]. Furthermore, the deployment of hydrogen-powered vehicles makes the study of electrostatic discharge hazards of primary importance. The energy E of a capacitive spark is defined as:

$$E = \frac{CV^2}{2} \quad (1)$$

where C is the capacitance and V is the applied voltage.

The MIE for hydrogen-air mixtures at ambient temperature has been widely investigated experimentally, e.g. Refs. [1,5,6]. Tests in Ref. [7] demonstrated that the MIE for hydrogen-air mixtures strongly depends on the gap distance between the electrodes, which was varied in the range 0.5–4 mm. It was observed that for near to stoichiometric composition, the MIE is achieved for the 0.5 mm gap. However, when changing the hydrogen content in the mixture, the MIE is achieved for different gap lengths. For instance, MIE for a mixture with 10% vol. Hydrogen in air is obtained for a gap equal to 2 mm, whereas for 50% hydrogen-air mixture the MIE is obtained for a gap of 1 mm. Similar dependence was found in Ref. [2] for mixtures enriched with oxygen (35% vol of oxygen in air) for electrodes' gap in the range 0.3–1 mm. The authors of [7] compared their MIE measurements with previous studies conducted in Refs. [1,5], observing up to twice deviation in MIE values measured for lean mixtures using different electrodes gap. The discrepancy was explained to be originated by differences in the experimental apparatus, such as the electrodes configuration (e.g., shape, gap, tip diameter, etc.) and material.

The effect of spark duration on the MIE was assessed in Ref. [7]. It was found that for a mixture with 22% vol. of hydrogen in air, the MIE did not present significant differences when the spark duration was varied in the range from 5 ns to 1 ms. The variation of initial temperature of the flammable mixture affects its capability to ignite and combustion characteristics. Semi-empirical correlations [8] give the increase of MIE for stoichiometric hydrogen-air mixtures to approximately 100 μJ at temperature 200 K. In 2022, Ghosh et al. [9] measured the MIE for 6.3% hydrogen-air mixture with temperature in the range 200–295 K. The MIE was seen to increase linearly from about 450 μJ at 295 K to about 1.2 mJ at 205 K. This experimental study confirmed the high variability of ignition energy for lean hydrogen-air mixtures at temperature lower than ambient. At 245 K the decrease in MIE by a factor of eight was observed when increasing hydrogen concentration in air from 6.3% to 7.7%.

There are several studies built on dependence of MIE on the quenching distance. In 1961, Lewis and von Elbe [1] assessed

the MIE dependence on the quenching distance and mixture temperature through their theoretical considerations. Their first equation considers the MIE as the amount of energy required to heat up a sphere of flammable mixture at initial temperature T_u of the unburnt mixture, to that of the flame, T_b. The quenching distance, d, is considered as the diameter of the critical flame kernel [1]:

$$E_{min} = \frac{1}{6}\pi d^3 \rho_b c_{p,av}(T_b - T_u) \quad (2)$$

where ρ_b is the density of the burnt mixture and $c_{p,av}$ is the heat capacity averaged between the fresh and burnt mixtures. Their second equation considers the minimum ignition energy to compensate the heat losses from the surface of the sphere heated by the released energy as [1]:

$$E_{min} = \pi d^2 \frac{k_{av}\ (T_b - T_u)}{S_u} \quad (3)$$

where k_{av} and S_u are the average heat conductivity and the burning velocity respectively. The authors found that for "strong" flames, E_{min} is proportional to d^3, whereas for "weaker" flames the proportionality was found to be as d^2 [1].

In 1986, Monakhov [10] reported that the MIE of flammable vapours and gases in the air expressed in millijoules may be calculated as $E_{min} = 0.01d^{2.5}$, where d is the critical extinguishing diameter, i.e. the quenching distance, expressed in millimetres.

In 2006, the proportionality of E_{min} to d^3 was stated by Law [11] based on the experimental results [5] for a variety of fuels including hydrogen. Law considered that the quenching distance should be of the same order of the laminar flame thickness δ_L, as this is the distance characterising heat losses. In this formulation, E_{min} is proportional to the amount of energy needed to heat up a spherical volume of unburnt mixture with density ρ_u and radius δ_L, from the unburnt mixture temperature T_u to that of the burnt mixture, assumed to be equal to the adiabatic flame temperature T_{ad} [11]:

$$E_{min} \sim \rho_u(\delta_L)^3 c_p(T_{ad} - T_u). \quad (4)$$

In 2007, Chen and Ju [12] investigated analytically and numerically the dynamics of flame kernel evolution with and without external energy addition. It was found that radiation losses affect the resulting flame regimes and increase significantly the critical ignition radius, which would determine the self-extinguishment of the flame or the successful ignition of the mixture. The results showed that the minimum ignition power would present three different dependencies on the Lewis number.

Despite theoretical considerations done in the past, the validated theoretical models to determine MIE in hydrogen-air mixtures at different concentrations and temperatures are still missing. The authors of [13] limited application of Eqs. (2) and (3) to only stoichiometric hydrogen-air mixture. They concluded that there is no relationship between quenching distance and laminar flame thickness, that is conversely to Ref. [11]. Furthermore, the previous models employed experimental data on quenching distance and laminar burning velocity. This would prevent the application of these models in conditions where experimental data are not available, such as mixtures with arbitrary hydrogen concentration and/or temperature. To overcome these uncertainties and shortcomings, the present study aims at developing a model for calculation of MIE requiring as input only hydrogen-air mixture composition and temperature. The study investigates the use of the laminar flame thickness to estimate the critical flame kernel. Cantera and Chemkin software are used to calculate the flame and mixtures parameters, and their performance is compared. To assess the validity of the correlation, results are compared against experiments described in Refs. [1,7] for the range of hydrogen concentration in air in the range 9–75% vol. With initial temperature equal to ambient. The applicability of the model is then extended to hydrogen-air mixtures formed by releases from storage and equipment at cryogenic temperature. The correlation is validated against unique experiments performed at INERIS facility within the Clean Hydrogen Joint Undertaking funded project "Pre-normative Research for Safe Use of Liquid Hydrogen" (PRESLHY, Grant Agreement No. 779613), where experiments were performed on hydrogen-air mixture with temperature in the range 123–293 K. Hydrogen-air mixtures at temperature below atmospheric can be formed during loss of liquid hydrogen containment or released from storage or equipment at cryogenic temperature (≤150 K [14]). The model can be applied to the entire range of temperatures of hydrogen-air mixtures from atmospheric down to lowest where gaseous mixture can exist without condensation of air components, i.e. 90 K (liquid oxygen boiling point). This is close to the model validation temperature domain of 123 K in the PRESLHY experiments.

Description of validation experiments

Hydrogen-air mixtures at ambient temperature

Validation data on MIE for hydrogen-air mixtures at ambient temperature are taken from three experimental campaigns, conducted in 1961 [1], 2007 [7] and 2020 [15] respectively. Conditions prior to ignition were ambient temperature and pressure. Earliest experiments [1] were conducted on hydrogen-air mixtures in the range of hydrogen concentrations in air 7–57% vol. The gap between electrodes was 0.5 mm. The MIE in Ref. [7] was measured using a capacitive spark discharge in a stainless-steel chamber of 1 L volume, and the tests were performed with 7–68% hydrogen-air mixtures. Needle to needle electrodes made of tungsten were used and located at the centre of the chamber. Fifty tests with gap between electrodes of 0.5 mm, 1 mm and 2 mm are selected for validation, as these test configurations provided the lower measurements of MIE. Spark duration was below 100 ns. Proust [15] proposed a technique to produce well controlled electrical sparks and promote reproducibility of tests. Transparent cylindrical chamber of 7 L volume was used to visualise the development of the spark and produced flame kernel. Tests were conducted for hydrogen concentration in air in the range 10–50% vol. The MIE measurements are reported in Table 1. These experiments were performed within the PRESLHY project for comparison with tests at cryogenic temperature, which are described in the following section.

Table 1 – *MIE for hydrogen-air mixtures at ambient [15] and cryogenic temperature (PRESLHY project).*

Hydrogen concentration in air (% vol.)	MIE at T = 298 K (μJ)	MIE at T = 173 K (μJ)
10	–	315.8
12	165.2	–
20	19.8	53.4
30	31.4	45.8
40	47.7	72.3
50	164.0	–

Hydrogen-air mixtures at cryogenic temperature

Tests on MIE measurements at cryogenic temperature were performed within the PRESLHY project [16]. The experimental set-up consisted of a vertical and tubular burner with height of 400 mm and diameter of 40 mm. The device was foam-insulated and filled with glass beads (Fig. 1). Liquid nitrogen was poured from the open top of the device into the glass beads to cool them down prior to the ignition tests. Three thermocouples at different heights of the burner were used to monitor the temperature within the system. The air and hydrogen were injected from the bottom of the burner and diffused in upward direction into the glass beads. The hydrogen-air mixture concentration was calibrated through mass flowmeters. The uniformity of concentration across and along the vertical burner were verified. The accuracy of concentration measurements was ±0.5% vol. The spark ignitor was located at the open top of the burner. The electrodes were made of tungsten of 0.1 mm diameter. The electrodes gap was fixed to 0.5 mm. A series of tests was performed at 173 K (−100 °C) for concentration of hydrogen in air equal to 10%, 20%, 30% and 40% vol. Table 1 reports a summary of the MIE measurements at 173 K (−100 °C). For example, the MIE for the 30% vol. of hydrogen in air was found to be 46 μJ Further experiments were conducted on hydrogen-air mixtures with concentration of 20%, 30% and 40% at variable initial temperature decreasing from ambient further down to 123 K (−150 °C) for the case of the 40% mixture. Results of this experimental campaign are shown in Fig. 12 along with the model predictions.

Analysis of MIE determination by existing quenching distance models [1]

The first attempt of MIE determination by Eqs. (2) and (3) was done in Ref. [13] with limitation to a stoichiometric hydrogen-air mixture at ambient temperature. Both equations resulted in MIE = 40 μJ [13], which is more than twice higher than the experimental measurements [1]. In the present study, Eqs. (2) and (3) are employed to calculate the ignition energy for mixtures with hydrogen concentration in air in the range 11–50% vol. as follows. Properties for the fresh and burnt mixtures were calculated through Cantera v.2.4.0. The quenching distance was retrieved from experimental data in Ref. [17], available for mixtures at ambient temperature with hydrogen content in air 11–50% vol., hence limiting the model calculation range. Burning velocity in Eq. (3) was calculated using the data on laminar burning velocity in Ref. [18]. Results are compared to experimental MIE in hydrogen-air mixtures [1,7,15] in Fig. 2. Equation (2) predicts well the MIE for a stoichiometric and rich mixtures. Predictions worsen for lean mixtures, possibly due to a less accurate determination of the quenching distance in experiments. Equation (3) results in lower calculated ignition energy, meaning that the energy needed to compensate the heat losses is lower than the energy required to heat up the fresh mixture to the flame temperature.

Despite the reasonable agreement of previous models with experiments for near-stoichiometric and rich mixtures (they still somewhat underpredict MIE for this range of concentrations), both models seriously overpredict the measured values of MIE for lean mixtures. This is unacceptable from safety point of view. Furthermore, these two equations employ experimental data for d and S_u which are currently available in literature only for mixtures at certain concentrations and temperatures, preventing the application of these two models for mixtures at arbitrary concentration and temperature.

Development and validation of the model for MIE determination

The former models presented by Eqs. (2) and (3) [1] are further developed here to calculate the MIE by knowing only initial temperature and composition of the hydrogen-air mixture. The model is validated against MIE experiments that are available at ambient pressure but is expected to reproduce MIE at higher pressures when they will be available. The variants of the model are summarised in Table 2. Firstly, Eq. (2) was modified to consider the density and specific heat of the unburnt mixture, as these are the properties determining the heat needed to bring a sphere of unburnt mixture with defined critical diameter to the adiabatic flame temperature (Models 1-B and 1-BS). The diameter of the critical flame kernel is considered to be proportional to the laminar flame front thickness similar to Ref. [11], see Eq. (4). It is reasonable to assume that a flame kernel should have a diameter of at least twice the laminar flame thickness to initiate the flame propagation. Babrauskas [19] analysed different literature sources and reported the quenching distance as $d = 2 - 2.2\delta_L$ or $d = 3.1\delta_L$, with δ_L being the laminar flame front thickness. The averaging of these expressions is employed here to calculate the critical flame kernel as:

$$d = 2.5\delta_L \tag{5}$$

The sections below show the assumptions and step by step procedure to calculate each of the parameters used in the revised Eqs. (2) and (3), i.e. the flame thickness, mixture properties and laminar burning velocity.

Laminar flame thickness

There are several ways to define the laminar flame thickness, δ_L, and a brief review as reported in Ref. [20] is provided here. A flame thickness can be retrieved from scaling laws. Following denomination in Ref. [20], this is called "diffusive" flame thickness, δ, and is defined as:

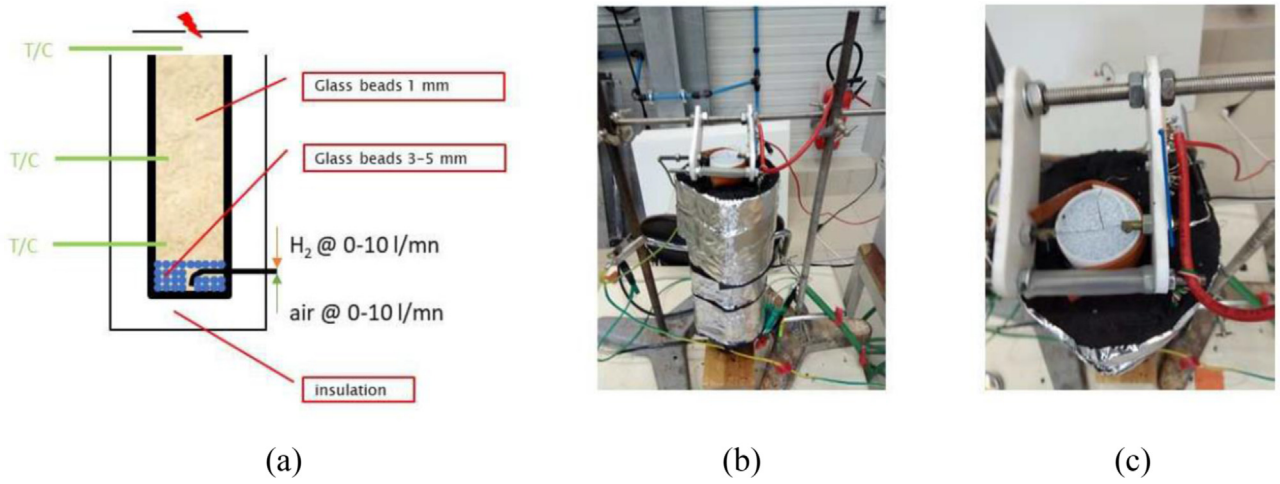

Fig. 1 – Burner configurations scheme (a) and photographs from the side (b) and top (c).

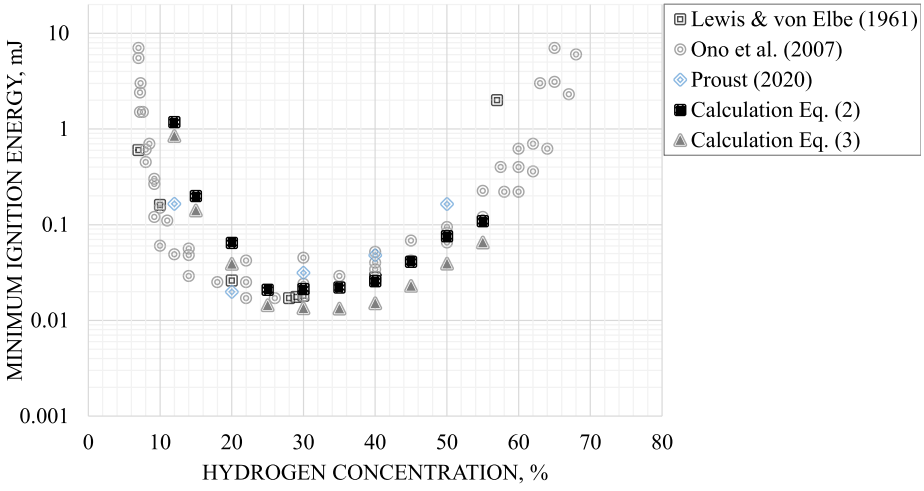

Fig. 2 – MIE calculated using previous quenching distance models (Eqs. (2) and (3) [1]) against experimental MIE [1,7,15].

Table 2 – Model variants for determination of MIE in hydrogen-air mixtures.

Model variant	MIE equation	Flame thickness equation
Model 1-B	$E_{min} = \frac{1}{6}\pi d^3 \rho_u c_{p,u}(T_b - T_u)$	$\delta_L^B = 2\delta \frac{k_b/c_{p,b}}{k_u/c_{p,u}}$
Model 2-B	$E_{min} = \pi d^2 \frac{k_{av}(T_b - T_u)}{S_u}$	$\delta_L^B = 2\delta \frac{k_b/c_{p,b}}{k_u/c_{p,u}}$
Model 1-BS	$E_{min} = \frac{1}{6}\pi d^3 \rho_u c_{p,u}(T_b - T_u)$	$\delta_L^{BS} = 2\delta\left(\frac{T_b}{T_u}\right)^{0.7}$
Model 2-BS	$E_{min} = \pi d^2 \frac{k_{av}(T_b - T_u)}{S_u}$	$\delta_L^{BS} = 2\delta\left(\frac{T_b}{T_u}\right)^{0.7}$

Note: relationship between "d" in the MIE equation (second column) and the flame thickness equation (third column) is given by Eq. (5).

$$\delta = \frac{k_u}{\rho_u c_{p,u} S_u} \tag{6}$$

where k_u is the thermal conductivity, ρ_u is the density, $c_{p,u}$ is the specific heat at constant pressure for unburnt mixture, and S_u is the laminar burning velocity.

A "thermal" flame front thickness is defined by the temperature gradient, it is considered to be more appropriate in Ref. [20]. This quantity is defined as:

$$\delta_L^0 = \frac{T_b - T_u}{max\left(\frac{\partial T}{\partial x}\right)} \tag{7}$$

Simpler correlations can be applied as the one proposed by Blint and reported in Ref. [20]:

$$\delta_L^B = 2\delta \frac{k_b/c_{p,b}}{k_u/c_{p,u}} \tag{8}$$

The equation may be further simplified by using the Sutherland law to estimate k and the assumptions of constant Prandtl number and c_p [20]:

$$\delta_L^{BS} = 2\delta\left(\frac{T_b}{T_u}\right)^{0.7} \quad (9)$$

The latter correlation requires only the knowledge of the temperature for the burnt mixture, which is easily obtainable from thermochemistry equilibrium calculations (see Section Parameters of unburnt and burnt mixtures). As reported by the authors [20], Eqs. (8) and (9) give a good estimation of δ_L^0. Furthermore, they allow to estimate the laminar flame thickness through parameters that could be computed by easily available software. Therefore, these two equations are employed for estimating δ_L in the calculation of the critical flame kernel diameter and their results are compared. For all calculations unless otherwise specified, the initial conditions of the hydrogen-air mixtures are ambient temperature (298 K) and pressure (1 atm). The flame kernel formation is assumed to be an isobaric process. In conclusion, four models resulting by the combination of two equations to calculate the MIE and two expressions to calculate the flame thickness are assessed and compared. The four model variants are summarised in Table 2 and the showed denomination will be used in figures comparing the results of their application. It should be noted that the laminar flame thickness may be also retrieved through the software mentioned in Section Parameters of unburnt and burnt mixtures. However, this approach is not pursued in the present study to allow extension of applicability of the model to lean and cryogenic hydrogen-air mixtures (see following sections).

Parameters of unburnt and burnt mixtures

Application of the models in Table 2 and calculation of the laminar flame thickness require the knowledge of the following thermophysical properties characterising the unburnt and burnt mixture: density, thermal conductivity, specific heat at constant pressure and temperature that is assumed to be the adiabatic flame temperature. These parameters are calculated through the equilibrium solver available in Cantera v.2.4.0 [21], assuming a constant pressure equal to 1 atm. Results are reported in Fig. 3 as a function of the hydrogen concentration in air. The use of either "mixture-averaged" or "multicomponent" transport models did not affect the results. The calculation of laminar burning velocity will be described in the following section.

The present work aims to develop a model applicable to cryogenic hydrogen-air mixtures as well. Cantera is used to calculate the thermophysical properties for the cryogenic mixtures, following the work [22] performed within the PRESLHY project, which used the STANJAN code [23] and Cantera [21] for the analysis of adiabatic combustion temperature in cryogenic hydrogen-air mixtures with temperature down to 78 K and 200 K, respectively. Fig. 4 reports the thermophysical properties for mixtures with initial temperature in the range 100–250 K. As expected, the largest effect of initial temperature is observable on the properties of the unburnt mixtures, especially density and thermal conductivity. The effect is less

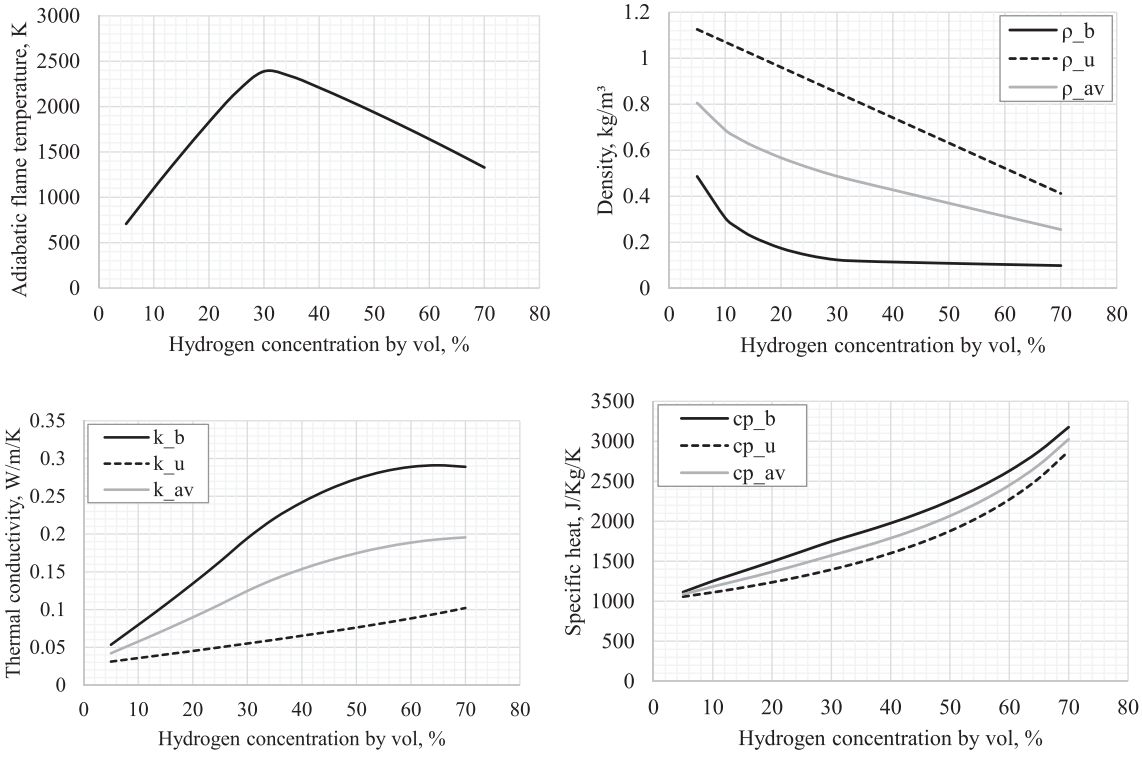

Fig. 3 – Thermophysical properties of the unburnt and burnt mixture as a function of hydrogen concentration in air for ambient temperature $T_u = 298$ K and atmospheric pressure.

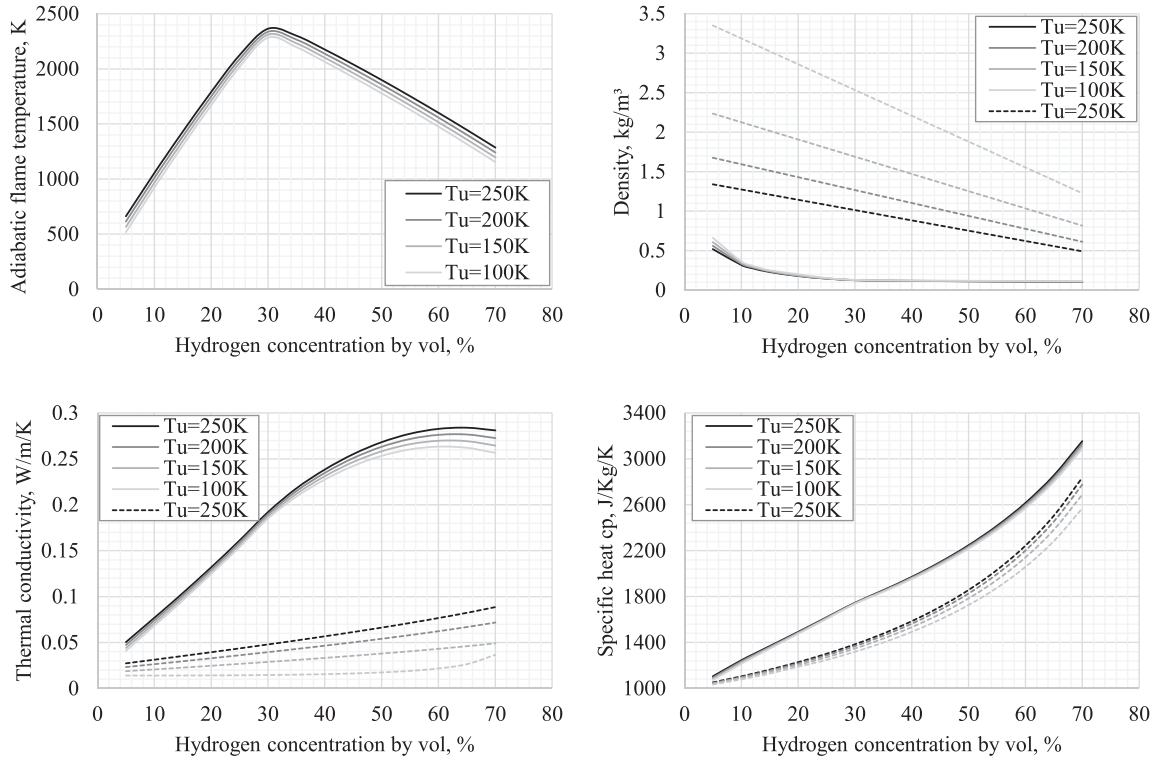

Fig. 4 – Thermophysical properties of the unburnt (dashed lines) and burnt mixture (solid lines) as a function of hydrogen concentration in air for the temperature range T_u = 100–250 K and atmospheric pressure.

pronounced for the properties of the burnt mixtures. When Cantera is not available for a user, Figs. 3 and 4 can be used to retrieve graphically the properties required to apply the model.

Laminar burning velocity

The laminar burning velocity is estimated through simulation of a freely propagating adiabatic one-dimensional (1D) flame in Cantera v.2.4.0 [21] employing GRI 3.0 chemical mechanisms. A uniform spatial grid of width 3 cm was specified for calculations, following the best practices [24]. Additional points are automatically added in the region with the steepest gradients according to the defined ratio, slope and curve. A sensitivity study was conducted on the parameters defining the refinement of the grid to ensure independency of the solution. The grid width was decreased to 1 cm, leading to a maximum difference of 3% for the mixture with hydrogen concentration in air 10% vol., whereas difference is unnoticeable for richer mixtures. The "ratio" parameter of Cantera determines the minimum spacing between grid points in simulations and if this value is exceeded, additional points will be added to the 1D grid. The "ratio" was decreased to the minimum possible, i.e., 2, from the default value of 10. Variation caused a negligible difference in results and calculation time. However, the ratio of 2 was maintained in the following simulations to achieve a better accuracy. The slope represents the maximum difference in value between two adjacent points. Default value is 0.06 and it can be varied in the range 0–1. The slope was decreased to 0.008, as lower values led to convergence issues. The decrease of slope caused a slight increase of laminar burning velocity for lean mixtures, and convergence was reached for a slope equal to 0.01, which was then applied for the follow-up calculations. The final tuning software parameter is the curve, which determines the maximum difference in the slope between two adjacent intervals. The curve value may be maximum 1. In the sensitivity study, the value was decreased to 0.03 and since no appreciable difference was noted in the results, a value of 0.09 was used for calculations to maintain a low computational time. Several studies reported dependence of the laminar burning velocity solution on the employed chemical mechanisms, especially for lean mixtures [25]. Thus, GRI 3.0 mechanisms were compared to Dryer's chemical mechanisms [25]. Results for GRI 3.0 and Dryer's mechanisms are reported in

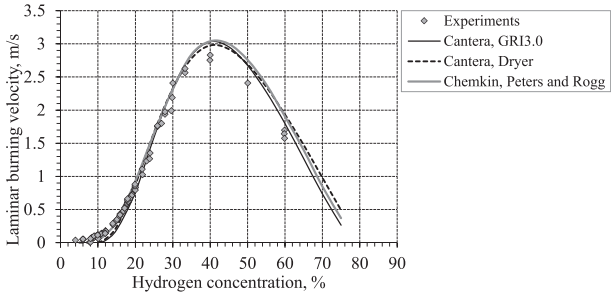

Fig. 5 – Laminar burning velocity calculated by Cantera and Chemkin software as a function of hydrogen concentration in air (T_u=298K): comparison of GRI3.0 [21], Dryer [25] and Peters and Rogg's [27] chemical mechanisms against experiments [18].

Fig. 5. In the second stage of the analysis, Chemkin software [26] was employed to estimate the laminar burning velocity for a freely propagating adiabatic 1D flame at atmospheric pressure. The laminar burning velocity, by definition, is calculated as the relative velocity between the unburnt gas mixture and the flame front. Detailed chemical mechanism considers a subset of Peters and Rogg's [27] mechanism with 18-step reduced chemical reaction mechanism for hydrogen combustion in air and 9 chemical specie. The numerical grid had a domain width of 10 cm and was not uniform, but it was adapted based on the temperature profile estimate: 1000 adaptive grid points were defined with maximum curvature equal to 0.5. The increase of adaptive grid points by two orders of magnitude and the decrease of maximum curvature to 0.2 presented a negligible difference in the results.

Fig. 5 shows the results of the laminar burning velocity calculations by Cantera [21] and Chemkin [26]. Results of laminar burning velocity computations are compared with data provided in Ref. [18] on unstretched laminar burning velocity retrieved from experiments. GRI3.0 mechanism resulted in a larger burning velocity for very lean mixture when compared to Dryer's mechanism employed in Cantera, reaching approximately 40% increase for the mixture with hydrogen content in air of 10% vol. On the other hand, calculations employing the subset by Peters and Rogg in Chemkin resulted in a larger laminar burning velocity by approximately 90% for the same hydrogen concentration (10%), with closer prediction of the experimental data. Thus, Chemkin has been selected for calculation of the laminar burning velocity further in the model.

Chemkin has been used to calculate the unstretched laminar burning velocity for the cryogenic hydrogen-air mixtures with temperature in the range 100–298 K. To confirm the validity of the theoretical calculations via the thermodynamic databases and chemical reaction mechanisms available in Chemkin, the calculated laminar burning velocity was compared to the processed experimental data for hydrogen-air mixtures with temperature in the range 100–300 K by Ref. [28], reported in Ref. [22]. Results have shown a good agreement for the mixtures with concentration equal or higher than stoichiometric, presenting a maximum variation of 12% for the mixtures at initial ambient temperature. The deviation between data by Ref. [28] and calculations in this study was seen to reduce with the decrease of temperature. The mixture with stoichiometric coefficient of 0.6 achieved a maximum deviation of about 30% at ambient temperature, whereas it decreased for lower temperatures of the mixture. Thus, it is concluded that Chemkin software with the available thermodynamic database and chemical reaction mechanism can still be used for the assessment of laminar burning velocity and MIE of cryogenic hydrogen-air mixtures.

Fig. 6 shows the results of calculation by Chemkin of the unstretched laminar burning velocity as a function of hydrogen concentration in air for initial temperature of the mixture in the range 100–298 K. This can be applied by a user to retrieve graphically the laminar burning velocity to be applied in the specific case.

The following equation is also used to assess the dependence of laminar burning velocity on mixture temperature at constant pressure [29]:

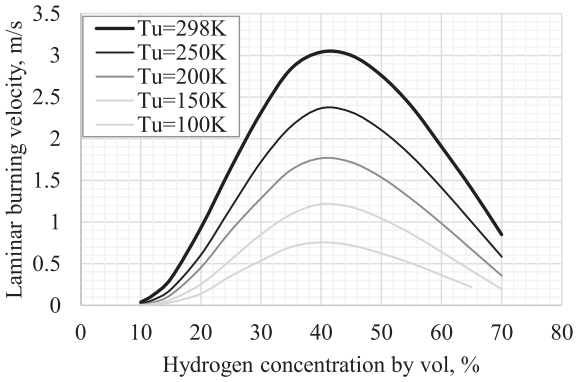

Fig. 6 – Unstretched laminar burning velocity calculated by Chemkin software as a function of hydrogen concentration in air and temperature of the unburnt hydrogen-air mixture at atmospheric pressure.

$$S_{u,T} = S_{u,ref} \cdot \left(\frac{T}{T_{ref}}\right)^{\alpha} \tag{10}$$

where $S_{u,ref}$ and T_{ref} are the laminar burning velocity and temperature at the reference state, here considered as the ambient conditions, and α is the temperature exponent. The authors of study [29] observed a decrease of α with the equivalence ratio, but nevertheless recorded a large scattering in results. The average value of $\alpha = 1.57$ was found for hydrogen-air mixtures with equivalence ratio in the range 0.5–1.0 and temperature 300–430 K. As reported in Ref. [29], this was found to be well comparable for the same range of concentration with $\alpha = 1.64$ reported in Ref. [30] for the temperature range of 293–523 K, and $\alpha = 1.53$ in Ref. [31] for the temperature range of 291–500 K. These values of α are comparable to the temperature exponent of 1.48 found for the maximum laminar burning velocity in Ref. [32] and the values reported in Ref. [22] for temperature lower than ambient. A constant exponent $\alpha = 1.48$ will be considered in the present study for hydrogen-air mixtures at temperatures below ambient. Nevertheless, it should be highlighted that α depends on the equivalence ratio, even if a strong scattering was observed for changing concentration of hydrogen in air [29].

Results and discussion

The model variants presented in Table 2 are applied to calculate MIE. Results are shown in Figs. 7 and 8 with legends following notation in Table 2. The calculations are limited to the range 9–70% vol. of hydrogen in air. Below 9% vol., the software used to calculate the laminar burning velocity does not reach a converged solution. Results of MIE calculations using "Blint" expression for a flame thickness are shown in Fig. 7. *Model 1-B* presents a good agreement with experimentally measured ignition energy but only for rich mixtures. The absolute minimum through hydrogen concentrations MIE is found to be 22.9 μJ for 35% hydrogen-air mixture, whereas for near-stochiometric 30% mixture MIE is equal to 29.3 μJ. These predictions correspond to the MIE of 17 μJ measured experimentally for the range of hydrogen concentrations in air 22–30% vol. On the other hand, performance of *Model 1-B*

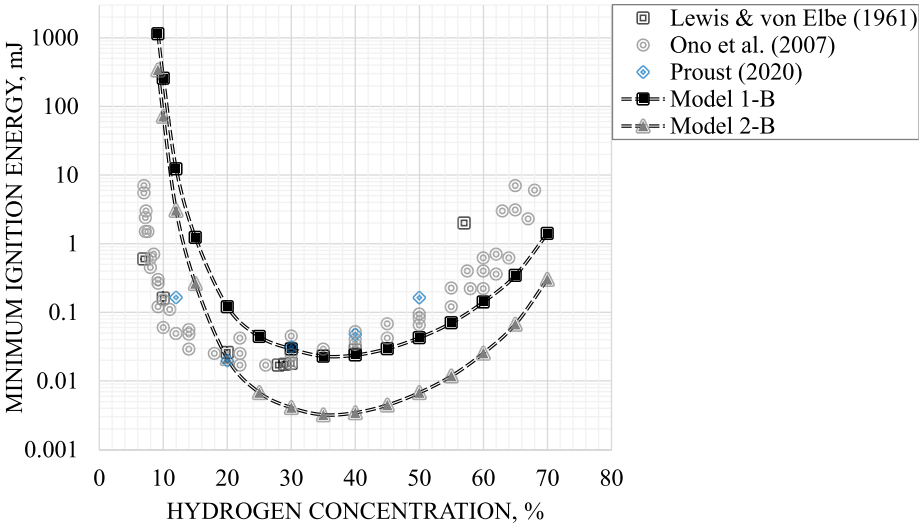

Fig. 7 – MIE calculation: experiments versus predictions of the models using "Blint" expression for the flame thickness.

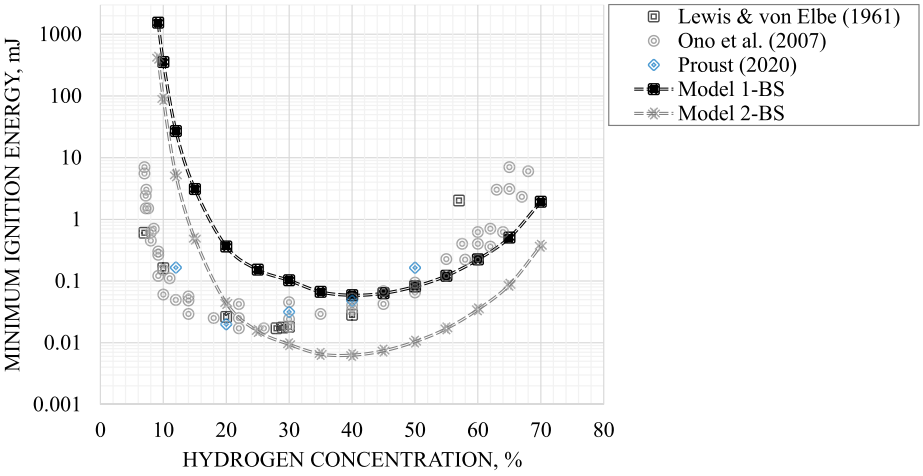

Fig. 8 – MIE calculation: experiments versus predictions of the models using "Blint-Sutherland" expression for the flame thickness.

deteriorates strongly for lean mixtures, overestimating the ignition energy by 3–4 orders of magnitude. *Models 1-B* and *2-B* give a larger difference in calculated MIE against measured MIE if compared to the two original Eqs. (2) and (3) presented in Fig. 2. This is mainly due to the use of the density and specific heat for unburnt mixtures in *Model 1-B*. *Model 2-B* presents a significant underestimation of MIE for the near-stoichiometric and rich mixtures, indicating probably that the energy losses through the surface of the flame kernel are potentially lower than the energy needed to heat the flame kernel from the initial temperature in the mixture to the adiabatic flame temperature, i.e. temperature of combustion products. The theoretical reasoning for *Model 1-B* is considered to be more valid for the problem under analysis and will be considered for the further development of the theoretical model for MIE determination in this study. This is in line with observation by Lewis and von Elbe's that for strong flames, such as hydrogen, the MIE shall be proportional to the cubic critical flame kernel diameter [1]. Yet, the poor performance of these models in the area of lean hydrogen-air mixtures is not acceptable and must be properly addressed.

Generally, the definition of flame thickness including the use of Sutherland law to calculate the mixture properties leads to a flame thickness larger than "pure" Blint definition. Consequently, the calculated MIE by either of the two theoretical models is higher (*Model 1-BS* and *Model 2-BS*). Fig. 8 shows the comparison between calculations and experiments. The absolute minimum of MIE for *Model 1-BS* is found to be 58.9 μJ for the rich 40% hydrogen-air mixture, whereas the absolute minimum of MIE in experiments is found to be 17 μJ in rather lean and near-stoichiometric range 22–30% vol. of hydrogen concentration in air [1,7,15]. Overall, definition of flame thickness by Blint, and thus *Model 1-B*, is considered to be more accurate, as it is free from calculation of properties

from the Sutherland law and the assumption of constant Prandtl number. Therefore, this definition will be employed for further model development.

Calculations of MIE employing *Model 1-B* were also performed by using the unstretched laminar burning velocity calculated through the Cantera software. In the range of hydrogen concentration in air 25–60% vol. The obtained MIE presented negligible variation from calculations using Chemkin laminar burning velocity. Outside this range, difference in calculations increased up to 50% for the 70% hydrogen-air mixture and to more than 90% for lean mixtures with hydrogen concentrations below 12% vol. The latter variation is due to a lower calculated unstretched laminar burning velocity by Cantera (thus resulting in higher MIE), which achieves an order of magnitude difference at hydrogen concentration in air 10% vol. This comparison supports the choice of Chemkin software for the unstretched laminar burning velocity calculations in the rest of this study.

Flame stretch and preferential diffusivity effects on the laminar burning velocity

Fig. 7 shows that *Model 1-B* represents the MIE curve well for rich hydrogen-air mixtures, whereas it overestimates it for lean mixtures. This is thought to be associated with the calculated laminar burning velocity, which is then used to calculate the flame thickness. Cantera and Chemkin software assume a 1D freely propagating premixed flat flame. Therefore, they allow calculation of the unstretched laminar burning velocity, hereby indicated as S_u^0. However, in 3D ignition process and outwards expanding flames, the local stretch due to the curvature and the strain rate cause the burning velocity to be different from that of a planar flame. Depending on the mixture composition, the spatial velocity will increase or decrease as the stretch is enhanced, as stated in Ref. [18].

Thermal-diffusive flame instability affects combustion rate depending on the effective Lewis number of the reactants. The combined effect of preferential diffusion and flame stretch may result in a local redistribution of the element mass fraction and enthalpy, leading to fuel enriched zones in a lean flame and resulting locally in more intense burning. Preferential diffusion was investigated in Ref. [33] for laminar counterflow flames. The authors observed a strong effect of preferential diffusion in blends with hydrogen, leading to significant changes of the flame structure and dynamics. On the other hand, preferential diffusion effects were found to be negligible for pure methane. Kishore et al. [34] reported as well that unstable flames were observed for lean mixtures of fuels with high hydrogen content due to preferential diffusion effects. The Markstein number represents the sensitivity of laminar burning velocities: if positive the flame is in a stable regime; otherwise (i.e., Ma<0) the flame is in the preferential diffusion instability regime. This is confirmed by experimental observations in Ref. [35], leading to the conclusion that a negative Markstein length indicates the flame surface is distorted due to thermal-diffusional instability causing acceleration of flame and formation of a cellular structure. The preferential diffusion of hydrogen in curved reaction zones, e.g. in conditions of turbulence generated by ignition source, is considered to be the mechanism of burning velocity increase through so-called leading points in lean mixtures [36]. Therefore, the combined effect of flame stretch and preferential diffusion causes the increase of burning velocity in lean hydrogen-air mixtures, which are in an unstable propagation regime. As cited in Ref. [34], Kwon and Faeth [37] indicated that the transition from unstable to stable regime is verified for a stoichiometric coefficient (Φ) equal to 0.6 in H_2–O_2-Ar mixtures. A hydrogen concentration of 24–26% by vol. ($\Phi \approx 0.8$) was found to be the limit for unstable-stable flame propagation in air [18]. This is approximately the hydrogen concentration limit below which *Model 1-B* worsen in prediction of the MIE curve, hinting that considering the unstretched laminar flame as calculated by Chemkin without inclusion of stretch effect and preferential diffusion may lead to underprediction of S_u and as consequence to overestimation of δ_L^B and MIE.

Lamourex et al. [18] determined experimentally the laminar burning velocity for spherical expanding flames in hydrogen mixtures with equivalence ratio in the range 0.28–3.75 (approximately 10–61% vol. of hydrogen in air). In the same study, the authors calculated the unstretched laminar burning velocity S_u^0 through a zero-stretch linear extrapolation. Alekseev et al. [38] collected data on the unstretched laminar burning velocity S_u^0 extrapolated by non-linear models for $\Phi = 0.3$–0.6. Data on the stretched laminar burning velocity taking into account preferential diffusion were given in Ref. [39] and are hereby indicated as S_u^{SD}. To include effects of both flame stretch and selective diffusion, a new parameter is calculated as the ratio of S_u^{SD} and the unstretched laminar burning velocity S_u^0 given by the dataset from Alekseev et al. [38] for hydrogen-air mixtures within the range of equivalence ratios $\Phi = 0.3$–0.6 (11–20% vol. of hydrogen in air) and data of Lamourex et al. [18] for equivalence ratios $\Phi = 0.6$–3.75 (20–61% vol. of hydrogen in air):

$$X_{SD} = \frac{S_u^{SD}}{S_u^0} \tag{11}$$

Results of the calculated factor X_{SD} are reported in Fig. 9 as a function of hydrogen concentration in the range 12–50% of hydrogen by volume in air ($\Phi = 0.32$–2.4) [18,38,39]. Factor X_{SD} has a steep rise as hydrogen concentration decreases in lean mixtures, reflecting on the increasing effect of stretch rate and selective diffusion. For hydrogen concentrations higher than 35%, the coefficient X_{SD} (triangles in Fig. 9) tends to the unity indicating that the combined effect of stretch rate and selective diffusion is negligible for rich mixtures, as also observed in Ref. [40].

The calculated factor X_{SD}, is compared in Fig. 9 with parameter $X_{exp,fit}$ fitting experimental data on MIE given in Refs. [1,7] and calculated as follows:

$$X_{exp,fit} = \frac{S_u^{exp,fit}}{S_u^0} \tag{12}$$

where S_u^0 is the unstretched laminar burning velocity calculated by Chemkin and $S_u^{exp,fit}$ is the laminar burning velocity retrieved from the experimental data by the inverse problem: experimental measurements of MIE [1,7] are used to calculate the critical flame kernel "*d*" through *Model 1-B* (see Table 2); once the critical flame kernel diameter is known, the laminar

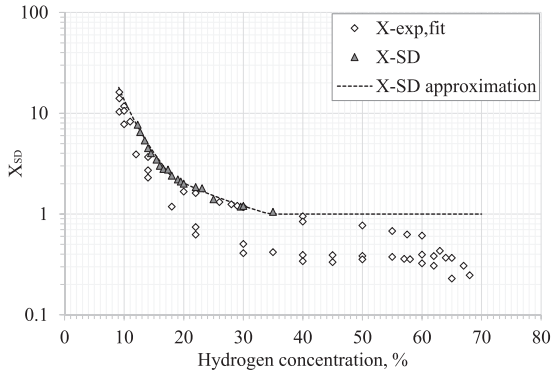

Fig. 9 – Factor X_{SD} accounting for the effect of flame stretch and preferential diffusion on laminar burning velocity as a function of hydrogen concentration: factor $X_{exp,fit}$ (white diamonds) fitting experimental data on MIE given in Refs. [1,7] and calculated as in Eq. (12); factor X_{SD} (grey triangles) calculated from experimental data on laminar burning velocity [18,38,39]; X_{SD} approximation (dashed black line) to be used in MIE calculation for arbitrary concentration according to Eq. (13).

flame thickness can be calculated from Eq. (5), $d = 2.5\delta_L^B$, and used in Eq. (8) to calculate the "diffusive" flame thickness, δ; finally, Eq. (6) is used to calculate the laminar burning velocity from δ calculated at the previous step as follows: $S_u^{exp,fit} = k_u/(\rho_u c_{p,u}\,\delta)$.

Fig. 9 shows that several values of factor $X_{exp,fit}$ may be attributed to the same hydrogen concentration. This is due to the fact that different values of MIE can be measured for the same concentration but different electrodes gap. Fig. 9 compares the estimated values of $X_{exp,fit}$, Eq. (12), against the introduced here factor X_{SD} calculated from data on laminar burning velocity [18,38,39]. It can be observed that factor X_{SD} agrees well with maximum values of factor $X_{exp,fit}$ up to the minimum concentration for which experimental data [18,38,39] are available (12% hydrogen-air mixture). To introduce factor X_{SD} in the MIE calculation for arbitrary concentration, three following functions of hydrogen concentration in air C_{H_2} are proposed:

$$\begin{cases} X_{SD} = 12980\cdot\left(C_{H_2}\right)^{-2.98} \text{ for } 9\% \le C_{H_2} < 20\%, \\ X_{SD} = 100\cdot\left(C_{H_2}\right)^{-1.30} \text{ for } 20\% \le C_{H_2} < 35\%, \\ X_{SD} = 1.0 \text{ for } C_{H_2} \ge 35\% \end{cases} \tag{13}$$

For rich hydrogen-air mixtures, $X_{SD} = 1$ is applied, following the distribution given by data available in literature [40], where it is explained that the effect of preferential diffusion of hydrogen compared to air in stretched flames is significant for the premixed combustion of lean hydrogen-air mixtures and it can be neglected for rich mixtures. The X_{SD} approximation is showed as black dashed lines in Fig. 9 and it is seen to correlate well with maximum values of factor $X_{exp,fit}$ calculated from experimental fit of MIE measurements, confirming the validity of the model down to the lowest concentration included in calculations (9% vol. of hydrogen in air).

The *Model 1-B* was expanded further to take into account the effect of flame stretch and selective diffusivity by using factor X_{SD} to correct the 1D unstretched laminar burning velocity calculated by Chemkin to real 3D cellular flame with wrinkles initiated at the electrodes gap. The calculated laminar burning velocity is then employed in Model 1-B to determine the corresponding laminar flame thickness (see Table 2). Fig. 10 compares MIE calculated by the model with and without factor X_{SD} with experimental MIE. Fig. 10 includes MIE measurement by Ref. [9] for a mixture of 6.3% hydrogen-air mixture for comparison with other experimental data by Refs. [1,7,15]. For rich mixtures with hydrogen concentration above 35% vol. There is no difference between prediction of MIE by previous models and developed in this study model, as expected, due to the fact that $X_{SD} = 1$ for this range of concentrations. The model agrees well with experiments, providing a conservative estimation of the MIE. In the

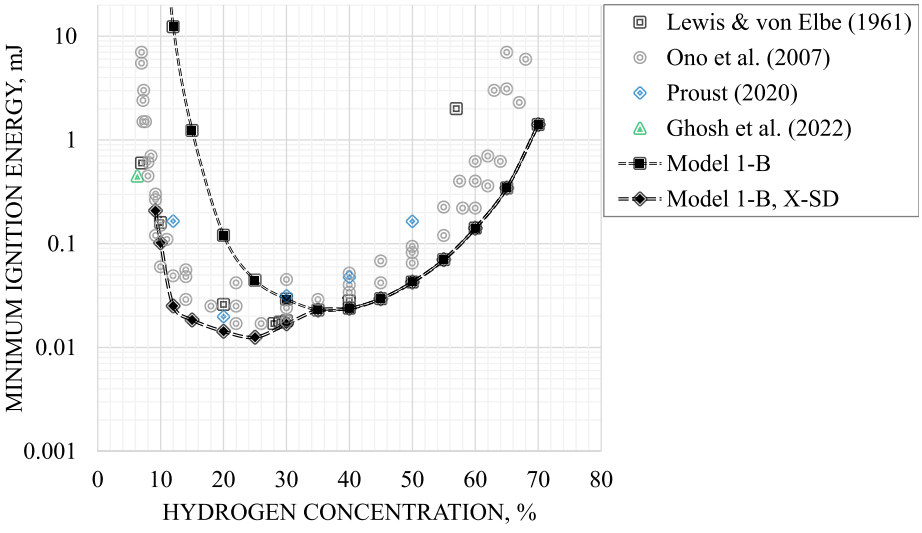

Fig. 10 – Experimental MIE data against calculations without (Model 1-B) and with (Model 1-B, X-SD) correction factor X_{SD} for flame stretch and preferential diffusion as a function of hydrogen concentration for ambient temperature ($T_u = 298$ K).

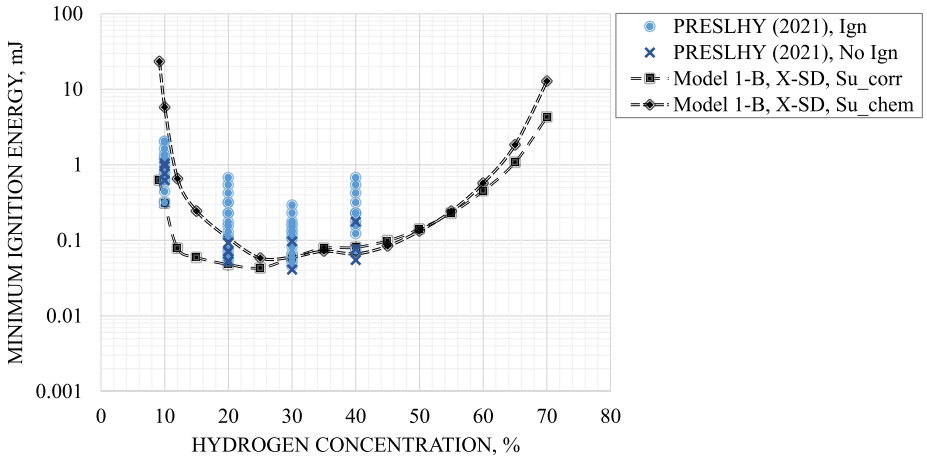

Fig. 11 – Comparison of results from the developed model using the laminar burning velocity calculated either by correlation of Eq. (10) (Model 1-B, X-SD, Su_corr) or by Chemkin software (Model 1-B, X-SD, Su_chem) against PRESLHY experiments on hydrogen-air mixtures at initial temperature 173 K.

proximity of 30% hydrogen concentration, the developed model presents an increase in the MIE curve following the experimental data. The MIE for the stoichiometric mixture is 13 μJ predicting well and conservatively the widely accepted in the literature value of 17 μJ. For hydrogen concentrations below 30% down to 9% vol., the model conservatively estimates the ignition energy, with exception of 10% hydrogen-air mixture where calculated value is somewhat higher than measured MIE. The somewhat deviation of the model predictions for very lean hydrogen-air mixtures below 10% vol. From experimental data may be associated to the following factors:

- Temperature of the flame is low and there could be more uncertainties in the employed chemical mechanisms [41];
- The onset of instabilities may occur earlier in the flame propagation, leading to a higher burning rate [41];
- The effect of flame stretch on the laminar burning velocity could also depend on the curvature of the flame relative to the flow;
- The model assumes spherical flame at constant pressure with a uniform stretch rate over the flame surface. This assumption may be inadequate for high energy discharges that generate turbulence that increase burning velocity further (not accounted in the current model).

Overall, the implementation of factor X_{SD} accounting for the effect of flame stretch and selective diffusion on the laminar burning velocity resolves the problem of poor predictive capabilities of *Model 1-B* for lean hydrogen-air mixtures. Thus, the developed model is found to predict well the MIE of hydrogen-air mixtures in the range of hydrogen concentration 9–70% vol.

MIE for hydrogen-air mixtures at temperatures below atmospheric

After validation against ambient temperature experiments, the developed model is applied firstly to reproduce tests at cryogenic temperature T_u = 173 K that were performed by INERIS within the PRESLHY project. Calculations in this section assume that the factor taking into account a flame stretch and selective diffusion, X_{SD}, does not depend on initial temperature. Fig. 11 compares the model predictions versus experimental results for the ignition energy leading to ignition (Ign) and to no ignition (No Ign) of a mixture. Two model curves are included in Fig. 11: "*Model 1-B, X-SD, S_{u_corr}*" that uses the correlation of Eq. (10) with $\alpha = 1.48$ to calculate the laminar burning velocity corrected by factor X_{SD} at temperatures below atmospheric; "*Model 1-B, X-SD, S_{u_chem}*" that uses Chemkin software for calculation of the laminar burning velocity at cryogenic temperature corrected by factor X_{SD}.

Firstly, the results for *Model 1-B, X-SD, S_{u_corr}* are discussed. The lowest MIE = 43 μJ is calculated for a 25% hydrogen-air mixture. The model reasonably reproduces the experimental lowest MIE = 46 μJ associated to the range of hydrogen concentrations 20–30% vol. For 40% hydrogen-air mixture, the model results are in a slight overestimation with MIE = 81 μJ compared to the measured in the experiments MIE = 72 μJ. The model is in excellent agreement with experimental measurements for 10% hydrogen-air mixture, resulting in a calculated 309 μJ versus 316 μJ recorded in the experiments. On the other hand, the *Model 1-B, X-SD, S_{u_chem}* is seen to overpredict experimental data for the lean hydrogen-air mixtures at 173 K, whereas it gives close prediction of MIE values for concentrations larger than stoichiometric.

It should be highlighted that for the experiments at 10% vol. of hydrogen in air and low temperature, it was found that small deviations in the hydrogen-air flow rate may results in large variations of MIE affecting the reliability of measurements. This could be the reason why a number of experimental tests resulting in the absence of ignition have a spark energy higher than the lowest recorded MIE of 316 μJ for the mixture with 10% hydrogen by vol. in air.

Fig. 12 compares the model predictions against PRESLHY experimental measurements for hydrogen-air mixtures with temperature in the range 123–293 K, and hydrogen concentration in air equal to 20%, 30% and 40% by volume. The general

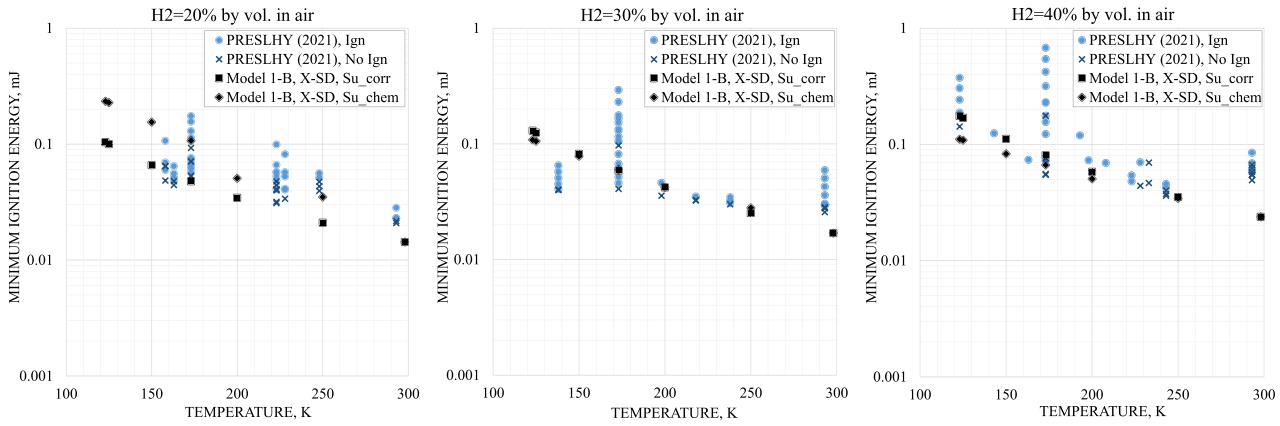

Fig. 12 – Comparison of results from the developed model using laminar burning velocity calculated either by correlation of Eq. (10) (Model 1-B, X-SD, Su_corr) or by Chemkin software (Model 1-B, X-SD, Su_chem) against PRESLHY experiments on hydrogen-air mixtures at initial temperature in the range 123–293 K and concentration of 20%, 30% and 40% vol. of hydrogen in air.

trend in experiments is the increase in MIE with the decrease of temperature. The decrease of initial temperature for the 20% hydrogen-air mixture from ambient 293 K–158 K leads to the increase of experimental MIE from 23 μJ to 60 μJ. For the 40% hydrogen-air mixture, the decrease of temperature from 293 K to 123 K leads to the increase of MIE from 58 μJ to 188 μJ.

Model 1-B, X-SD, S_{u_corr} predictions agree well with the experimental trend. On the other hand, predictions are seen to somewhat overestimate the experimental measurements for the 30% hydrogen-air mixture at temperature below 200 K. This could be related to the model assumption on the independence of factor X_{SD} responsible for flame stretch and preferential diffusion on temperature. This could be considered for the further development of the model when more experimental data on burning velocity in a wider range of temperatures below atmospheric would be available.

The lowest temperature used in experiments was 123 K and measurements are available only for 40% hydrogen-air mixture with MIE = 188 μJ, which is conservatively estimated by the model MIE = 175 μJ. Fig. 12 shows that the lowest MIE = 104 μJ at 123 K is calculated by *Model 1-B, X-SD,* S_{u_corr} for 20% hydrogen-air mixture. The application of the model for mixture at temperature 100 K results in further increase of lowest MIE to 153 μJ. It is recommended to handle carefully results obtained below 100 K due to the condensation of the air components starting from oxygen at 90 K.

Model 1-B, X-SD, S_{u_chem} predictions result in a poorer agreement with experimental data, signalling that correlation in Eq. (10) with temperature exponent retrieved for cryogenic hydrogen-air mixture may be more accurate in the estimation of laminar burning velocity compared to Chemkin software for the selected chemical mechanism. For 20% hydrogen-air mixture, *Model 1-B, X-SD,* S_{u_chem} shows a steeper increase of MIE with the decrease of temperature, resulting at 123 K in about twice the MIE calculated by the model employing correlation of Eq. (10). On the other hand, for hydrogen concentration equal to 30% and 40%, *Model 1-B, X-SD,* S_{u_chem} results in a slightly lower MIE.

Table 3 – The developed model and calculation procedure for the determination of MIE of hydrogen-air mixtures for known hydrogen concentration, C_{H_2}, and initial mixture temperature, T_u.

Step	Parameter to be calculated	Calculation tool or equation
1	Unstretched laminar burning velocity, S_u^0	"Freely propagating adiabatic 1D flame" solver in Chemkin or Fig. 6 or Eq. (10) if $T < T_{amb}$
2	Parameter accounting for the effect of flame stretch and preferential diffusion on the laminar burning velocity, X_{SD}	For 9%≤ C_{H_2} ≤20%: $X_{SD} = 12980 \cdot (C_{H_2})^{-2.98}$ For 20%≤ C_{H_2} <35%: $X_{SD} = 100 \cdot (C_{H_2})^{-1.30}$ For C_{H_2} ≥35%: $X_{SD} = 1.0$
3	Stretched laminar burning velocity, S_u^{SD}	$S_u^{SD} = X_{SD} \cdot S_u^0$
4	Thermophysical properties for the unburnt and burnt mixture: ρ_u, k_u, k_b, $c_{p,u}$, $c_{p,b}$, T_b	Equilibrium solver available in Cantera v.2.4.0 or Figs. 3 and 4
5	Diffusive laminar flame thickness, δ	Eq. (6): $\delta = \frac{k_u}{\rho_u c_{p,u} S_u^{SD}}$
6	Laminar flame thickness calculated using Blint definition, δ_L^B	Eq. (8): $\delta_L^B = 2\delta \frac{k_b/c_{p,b}}{k_u/c_{p,u}}$
7	Diameter of the critical flame kernel, d	Eq. (5): $d = 2.5\delta_L^B$
8	Minimum ignition energy, E_{min}	Table 2 - *Model 1-B*: $E_{min} = \frac{1}{6}\pi d^3 \rho_u c_{p,u}(T_b - T_u)$

Given the observed increase of MIE with the decrease of temperature, it can be recommended in practice that the safety measures and guidelines indicated for ambient temperature mixtures can be applied for cryogenic hydrogen-air mixtures [42]. Table 3 summarises the full procedure and equations of the developed and validated model for the calculation of MIE in hydrogen-air mixtures at temperature equal to and below atmospheric.

Conclusions

The significance of this study is in the capability of the developed and validated model to be used as a contemporary hydrogen safety engineering tool to assess the ignition potential of hydrogen-air mixture by calculation of MIE for arbitrary hydrogen concentration in air and mixture temperature. The developed model for MIE employs the laminar flame thickness to calculate the critical flame kernel needed for a spark ignition of hydrogen-air mixture. It does not require the performance of experiments on quenching distance as a critical flame kernel and laminar burning velocity as in former models that was a serious limiting factor for their use in hydrogen safety engineering. The experimental data required by previous models are limited and available only for mixtures at certain concentrations and initial conditions, preventing the application of those models to mixtures at cryogenic temperatures and arbitrary concentration.

The originality of the developed model is in the inclusion of the flame stretch and preferential diffusion effects on laminar burning velocity which is beyond the current capabilities of Cantera and Chemkin software. This feature of the model allows to reproduce available experimental MIE in the range 9–70% vol. of hydrogen in air, including the challenging lean mixtures, that was not possible before.

The rigour of the research is underpinned by the validation of the model against experiments at ambient temperature from multiple sources. The model reproduces experimental data on MIE of hydrogen-air mixtures within the concentration range of 9–70% vol. of hydrogen in air, and the theoretical lowest MIE = 13 μJ is close to the widely accepted MIE = 17 μJ measured for near-stoichiometric hydrogen-air mixtures. The model validation domain is extended to cryogenic mixtures at temperatures down to 123 K by the comparison against unique experimental data obtained within the PRESLHY project. It is demonstrated that the calculation of MIE by using the dependency of laminar burning velocity on temperature with exponent $\alpha = 1.48$ can accurately represent experimental measurements at temperatures below atmospheric down to cryogenic temperatures. The decrease of temperature from ambient 298 K–173 K leads to the increase of experimental MIE from 17 μJ to about 46 μJ. This increase in measured MIE is well reproduced by the model (43 μJ). The calculated MIE = 175 μJ conservatively estimates the experimentally measured MIE = 188 μJ at the lowest tested temperature of 123 K for the 40% hydrogen-air mixture.

Declaration of competing interest

The authors declare that they have no known competing financial interests or personal relationships that could have appeared to influence the work reported in this paper.

Acknowledgments

The authors are grateful to Professor A. N. Lipatnikov for sharing his expertise on the calculation of combustion properties for hydrogen-air mixtures and valuable discussions. This research has received funding from the Fuel Cells and Hydrogen 2 Joint Undertaking (now Clean Hydrogen Partnership) under the European Union's Horizon 2020 research and innovation programme under grant agreement No. 779613 (PRESLHY) and No.736648 (NET-Tools). This Joint Undertaking receives support from the European Union's Horizon 2020 research and innovation programme, Hydrogen Europe and Hydrogen Europe Research.

REFERENCES

[1] Lewis B, von Elbe G. Combustion, flames and explosions of gases, vol. 36. New York: Academic Press; 1961. https://doi.org/10.1524/zpch.1963.36.3_4.136.
[2] Kumamoto A, Iseki H, Ono R, Oda T. Measurement of minimum ignition energy in hydrogen-oxygen-nitrogen premixed gas by spark discharge. J Phys Conf Ser 2011;301. https://doi.org/10.1088/1742-6596/301/1/012039.
[3] Kuchta JM. Investigation of fire and explosion accidents in the chemical, mining, and fuel-related industries A manual, vol. 680. US Bur Mines Bull; 1985.
[4] Pratt TH. Electrostatic ignitions of fires and explosions. New York, NY: Center for Chemical Process Safety of the American Institute of Chemical Engineer; 2000.
[5] Calcote HF, Gregory CA, Barnett CM, Gilmer RB. Spark ignition. Effect of molecular structure. Ind Eng Chem 1952;44:2656–62. https://doi.org/10.1021/ie50515a048.
[6] Rose HE, Priede T. Ignition phenomena in hydrogen-air mixtures. Symp. Combust. 1958;7:436–45.
[7] Ono R, Nifuku M, Fujiwara S, Horiguchi S, Oda T. Minimum ignition energy of hydrogen-air mixture: effects of humidity and spark duration. J Electrost 2007;65:87–93. https://doi.org/10.1016/j.elstat.2006.07.004.
[8] Martín-Valdepeñas JM, Jiménez MA. Exploring MIE as a safety indicator parameter in practical applications. 2003.
[9] Ghosh A, Munoz-munoz NM, Lacoste DA. Minimum ignition energy of hydrogen-air and methane-air mixtures at temperatures as low as 200 K. Int J Hydrogen Energy 2022;47:30653–9. https://doi.org/10.1016/j.ijhydene.2022.07.017.
[10] Monakhov VT. Methods for studying the flammability of substances. Amerind Publishing Co.; 1986.
[11] Law CK. Combustion physics. Cambridge University Press; 2006.
[12] Chen Z, Ju Y. Theoretical analysis of the evolution from ignition kernel to flame ball and planar flame. Combust Theor Model 2007;11:427–53. https://doi.org/10.1080/13647830600999850.

[13] Kondo S, Takahashi A, Tokuhashi K. Calculation of minimum ignition energy of premixed gases. J Hazard Mater 2003;103:11–23. https://doi.org/10.1016/S0304-3894(03)00226-7.
[14] Office of Energy Efficiency & Renewable. Physical hydrogen storage. 2022. https://www.energy.gov/eere/fuelcells/physical-hydrogen-storage.
[15] Proust C. A new technique to produce well controlled electrical sparks. Application to MIE measurements. In: 13th int. Symp. Hazards. Braunschweig, Germany: Prev. Mitig. Ind. Explos.; 2020.
[16] Proust C, Jamois D. Some fundamental combustion properties of "cryogenic" premixed hydrogen air flames. Edinburgh, Scotland, UK: ID32. Int. Conf. Hydrog. Saf.; 2021. p. 1–12.
[17] Kim HJ, Hong SW, Kim HD. Quenching distance measurement for the control of hydrogen explosion. Int. Colloq. Dyn. Explos. React. Syst. 2001:1–5.
[18] Lamoureux N, Djebaili-Chaumeix N, Paillard CE. Laminar flame velocity determination for H2-air-stream mixtures using the spherical bomb method. J Phys 2002;12:445–58.
[19] Babrauskas V. Ignition handbook. Issaquah WA, USA: Society of Fire Protection Engineers, Fire Science Publishers; 2003.
[20] Poinsot T, Veynante D. Theoretical and numerical combustion. 2nd ed. Second. Philadelphia, PA, USA: Inc., P.O.; 2005. https://doi.org/10.1016/j.dss.2003.08.004. R.T. Edwards.
[21] Goodwin DG, Moffat HK, Schoegl I, Speth RL, Weber BW. Cantera: An object-oriented software toolkit for chemical kinetics, thermodynamics, and transport processes. V 2.4.0. 2021. https://doi.org/doi:10.5281/zenodo.6387882.
[22] Kuznetsov M. PRESLHY Deliverable 5.1. Theory and analysis of combustion of pre-mixed systems with cryogenic hydrogen. PRESLHY Proj; 2020.
[23] Reynolds WC. STANJAN: interactive computer programs for chemical equilibrium analysis. 1981.
[24] Felden A. Cantera Tutorials - a series of tutorials to get started with the python interface of cantera. 2015. Cerfacs.
[25] Lipatnikov A. Private communication. 2018.
[26] CHEMKIN. Reaction Design: San Diego. 2011.
[27] Peters N, Rogg B. Reduced kinetic mechanisms for applications in combustion systems. 1993. Berlin. Berlin.
[28] Bavoil E. Etude expérimentale de l'influence de la diminution de la température initiale (jusqu'à 100K) sur les déflagrations des mélanges H2-air. 1997.
[29] Verhelst S, Woolley R, Lawes M, Sierens R. Laminar and unstable burning velocities and Markstein lengths of hydrogen-air mixtures at engine-like conditions. Proc Combust Inst 2005:209–16.
[30] Liu DDS, MacFarlane R. Laminar burning velocities of hydrogen-air and hydrogen-air steam flames. Combust Flame 1983;49:59–71.
[31] Iijima T, Takeno T. Effects of temperature and pressure on burning velocity. Combust Flame 1983;65:35–43.
[32] Cirrone D, Makarov D, Molkov V, Venetsanos A, Coldrick S, Atkinson G, et al. Detailed description of novel engineering correlations and tools for LH2 safety, version 2. PRESLHY project Deliverable D6 2021;5.
[33] van Oijen JA, Bastiaans RJM, Goey de Lph. Modelling preferential diffusion effects in premixed methane-hydrogen-air flames by using flamelet-generated manifolds. Lisbon: Fifth Eur Conf Comput Fluid Dyn ECCOMAS CFD; 2010. Port June 2010:1–12.
[34] Kishore VR, Ravi MR, Ray A. Effect of hydrogen content and dilution on laminar burning velocity and stability characteristics of producer gas-air mixtures. Int J React Syst 2008;2008:1–8. https://doi.org/10.1155/2008/310740.
[35] Kuznetsov M, Kobelt S, Grune J, Jordan T. Flammability limits and laminar flame speed of hydrogen-air mixtures at sub-atmospheric pressures. Int J Hydrogen Energy 2012;37:17580–8. https://doi.org/10.1016/j.ijhydene.2012.05.049.
[36] Lipatnikov AN, Chomiak J. Molecular transport effects on turbulent flame propagation and structure. Prog Energy Combust Sci 2005;31:1–73. https://doi.org/10.1016/j.pecs.2004.07.001.
[37] Kwon OC, Faeth GM. Flame/stretch interactions of premixed hydrogen-fueled flames: measurements and predictions. Combust Flame 2001;124:590–610.
[38] Alekseev VA, Christensen M, Berrocal E, Nilsson EJK, Konnov AA. Laminar premixed flat non-stretched lean flames of hydrogen in air. Combust Flame 2015;162:4063–74.
[39] Zimont VL, Lipatnikov AN. A numerical model of premixed turbulent combustion of gases. Chem Phys Reports 1995;14:993–1025.
[40] Molkov V, Bragin M. Hydrogen-air deflagrations: vent sizing correlation for low-strength equipment and buildings. Int J Hydrogen Energy 2015;40:1256–66. https://doi.org/10.1016/j.ijhydene.2014.11.067.
[41] Bane SPM, Ziegler JL, Boettcher PA, Coronel SA, Shepherd JE. Experimental investigation of spark ignition energy in kerosene, hexane, and hydrogen. J Loss Prev Process Ind 2013;26:290–4. https://doi.org/10.1016/j.jlp.2011.03.007.
[42] Bernard L, Houssin D, Jallais S, Jordan T, Cirrone D. Novel guidelines for safe design and operation of LH2 systems and infrastructure, vol. 2. PRESLHY Project Deliverable D6; 2021.